Engineering Thermodynamic Approach to the Analysis of Elastic Properties: Elastomers as a Case Study

applied sciences

MDPI

Communication

Engineering Thermodynamic Approach to the Analysis of Elastic Properties: Elastomers as a Case Study

Umberto Lucia [1,3,*] and Giulia Grisolia [2,3,*]

[1] Dipartimento Energia "Galileo Ferraris", Politecnico di Torino, Corso Duca degli Abruzzi 24, 10129 Torino, Italy
[2] Dipartimento di Ingegneria dell'Ambiente, del Territorio e delle Infrastrutture, Politecnico di Torino, Corso Duca degli Abruzzi 24, 10129 Torino, Italy
[3] INFN—Sezione di Torino, 10129 Torino, Italy
* Correspondence: umberto.lucia@polito.it (U.L.); giulia.grisolia@polito.it (G.G.); Tel.: +39-011-090-4558 (U.L.)

Abstract

The thermophysical behavior of solids (such as oxide compounds, for example) is crucial in applied physics and engineering, with particular regard to heterogeneous catalysis, sensors, high-temperature superconductors, and solid-state batteries. Research in geometric nonlinear theory has provided insights into crystal symmetry and phase compatibility under thermal and elastic stress. High-temperature stress significantly affects phase stability, making an understanding of solid thermodynamics essential for material performance. This study focuses on the mechanical and thermal interactions in solids, analyzing variations in mechanical stress and strain under extreme conditions. We propose a theoretical approach for a thermophysical model that, based on the study of the properties of the global thermal behavior of solids, can describe the thermodynamic effects of elastic deformations. Elastomers are used as a case study to validate the proposed approach.

Keywords: thermodynamics; thermoelasticity; strain–stress modelling; elastomers

Academic Editor: José A. Orosa

Received: 17 July 2025
Revised: 31 July 2025
Accepted: 3 August 2025
Published: 6 August 2025

Citation: Lucia, U.; Grisolia, G. Engineering Thermodynamic Approach to the Analysis of Elastic Properties: Elastomers as a Case Study. *Appl. Sci.* **2025**, *15*, 8705. https://doi.org/10.3390/app15158705

1. Introduction

Materials science and engineering drive technological innovation across industries through advanced materials and applications [1]. Materials science market research focuses on material properties, structure, and applications, enabling efficient and durable products that enhance the quality of life. As industries innovate, demand for skilled materials scientists grows, stimulating economic development [1]. Companies investing in materials research gain competitiveness through innovation. Advanced materials use drives leadership in green materials, additive manufacturing, smart and functional materials, nanomaterials, and biomaterials.

The driving factors of the materials science market can be summarized as:

- Technological advancements: due to evolving needs in electronics, healthcare, aerospace, and automotive; they require high-performance materials to maintain competitiveness [1];
- Sustainability: environmental concerns drive the development of sustainable materials like biodegradable plastics, recyclables, and bio-based alternatives [2];
- Emerging technologies: new technologies require materials that enhance performance, accelerating market growth [1].

Tailor-made materials result from advances in structure–property theory, characterization, and control of advanced manufacturing (e.g., nanotechnology, molecular and surface engineering). While lab identification of suitable materials is often feasible, scaling up manufacturing remains a major challenge. Moreover, mathematical-statistical modelling improves efficiency in material and process design.

Understanding the thermophysical behavior of solids is essential for engineering design, particularly under high temperatures, where phase stability is critical. However, studies on the mechanical performance of advanced structural materials remain limited. Furthermore, fatigue cracks have been a key factor in structural failures for two centuries [3]. The use of fracture mechanics has improved structural efficiency, avoiding premature decommissioning and reducing costs. However, aspects like crack closure remain poorly understood, primarily due to difficulties in evaluating their effect on the crack driving force [4].

Recently, there has been a notable increase in research on the interaction between mechanical and thermal effects in solid materials [5]; driven by the development of advanced materials (e.g., ceramics, composites), researchers now emphasize time, temperature, and scale phenomena, beyond purely mechanical aspects [6]. For metals and alloys, extensive studies have explored temperature–strain relationships based on thermodynamic laws [5], extending to concrete and mortar via analyses of Grüneisen parameters, heat diffusivity, and thermal expansion [7]. Improved measurement tools have advanced non-destructive structural testing by enabling surface heat emission analysis [8,9]. In the elastic regime, challenges include incorporating principal stresses under thermal changes and using the linear stress tensor in 2D and 3D bodies [10,11]. In inelastic analyses, attention centers on dissipation phenomena preceding failure [5]. Most theoretical models assume absolute zero temperature and a perfect and fixed crystalline arrangement of atoms, offering insights under low stress and temperature, but for engineering purposes, it is more relevant to investigate solids at ambient temperature under high external loads [12–14].

Thermomechanical interactions in solids are of growing interest due to their engineering relevance and insight into material thermophysical behavior. The theory of thermoelasticity combines principles of elasticity and heat conduction. It relates to how heat affects the deformation of an elastic medium and how deformation, in turn, influences the medium's thermal state. Thermal stress arises when the rate of change in heat sources or boundary conditions in a medium is compared with the medium's structural oscillation characteristics. In such cases, solutions for temperature and stress distributions should be derived using the coupled thermoelasticity equations. It should be noted that the classical theory presents an uncoupled view of thermoelasticity, which does not accurately reflect the physical behavior of the medium. In classical theory, the thermal equation takes a parabolic form, implying infinite speeds for heat wave propagation—a notion that is physically impossible, particularly in scenarios involving thermal shocks. Over the past decade, several non-classical theories have been developed to address these issues. These theories propose modifications to Fourier's law of heat conduction, incorporating hyperbolic heat transfer equations that account for finite thermal pulse velocities. According to these models, thermal propagation can be regarded as a wave phenomenon rather than a diffusion process [15].

The recent years have highlighted that the investigation into the mechanical behavior of high-tech materials for structural uses is often insufficient. Consequently, research on the interplay between mechanical and thermal effects in solid materials has garnered significant attention.

The hyperbolic form refers to the finite velocities of heat distributions, known as second sound, which was first introduced by Maxwell [16]. This second sound phenomenon

allows for finite speeds in thermoelastic wave propagation, particularly in situations involving thermal shocks, in contrast to the implications of Fourier's law, which suggests that waves travel through a body without delay, which is not realistic. In 1967, Lord and Shulman [17] proposed a wave-form thermal equation, suggesting a new approach to heat conduction that deviates from Fourier's law. They introduced the concept of relaxation time, and their theory indicates a linear relationship between temperature and heat flux that incorporates both the rate of temperature change and the thermal rate [15]. Green and Lindsay [18] expanded this concept in 1972, presenting a second generalized theory where the temperature rate is treated as a dependent variable influenced by two distinct relaxation times. They also established two separate lag times within the entropy expression and the correlation of stress [15].

Green and Naghdi [19] introduced a new model that does not take energy wastage into account, utilizing the displacement-temperature-flux rate in Fourier's law. Unlike the classical heat conduction model that adheres to Fourier's law, a key feature of this new model is its exclusion of energy loss. In their theory, Green and Naghdi put forward three distinct forms of constitutive response functions [15].

Recently, non-destructive analysis has emerged as a fundamental requirement for experimental applications, with the need to be based on simple analytical methods. Thus, non-destructive stress analysis, referred to as the thermoelastic effect, has emerged as an effective method for engineering and industrial stress analysis. In [13,14], a theoretical framework for the thermoelastic effect has been developed, offering a simple mathematical model to support the interpretation of non-destructive analysis experimental results only limited to SPATE (Stress Pattern Analysis by the measurement of Thermal Emission), i.e., an equipment for the radiometric monitoring of the temperature changes induced by cyclic loading in the elastic range. This paper aims to generalize the thermophysical approach, achieving a model for the measurement of thermophysical properties of materials under experimental techniques that are not necessarily periodic. To do so, we utilize the intrinsic formulation of linear thermoelasticity theory [20], linking temperature changes to stress variation, under some theoretical approximation; indeed, the outcome is influenced by the first and second invariants of stress, whereas the second invariant becomes negligible when there is only one principal stress component. In summary, we develop a theoretical model describing thermal effects on elastic behavior. To do so, in Section 2 the theoretical approach is developed. In Section 3, the previous general results are used in the analysis of elastomer behavior as a case study, and a comparison with experimental results in the literature is developed to validate the approach. In Section 4, some considerations are introduced, and in Section 5 a summary of the results obtained is proposed. The preliminary result presented consists of a simplified approach for engineering applications to evaluate the thermophysical properties of elastomers for industrial use. Elastomers are considered to be a case study; indeed, they are essential in engineering due to their unique combination of properties, including high elasticity, flexibility, durability, and resistance to various environmental factors. They are used in a wide range of applications, from vibration dampening to seals and gaskets, and play a vital role in industries like automotive, aerospace, and oil and gas. Their thermophysical properties are crucial for understanding their behavior in various applications, particularly regarding their performance under different temperature conditions. Understanding these properties helps predict how elastomers will react when exposed to changes in temperature, impacting their function and longevity.

2. Materials and Methods

In this Section, we develop the theoretical bases of the thermophysical model proposed. To do so, we consider a continuum elastic body [13,14,21]. It has been assumed that the

bounded regular region of space, occupied by the body in a fixed reference configuration, is, respectively, closed in the case of mass transfer and opened in the case of energy transfer. This body is defined as a thermodynamic closed system. According to Carlson [20], the local form of the First Law of Thermodynamics can be written as:

$$\rho\,\dot{e} = \hat{\mathbf{S}} \cdot \dot{\mathbf{F}} - \nabla \cdot \mathbf{q} + \rho\, r \tag{1}$$

where ρ is the mass density, r represents the heat supply per unit mass and unit time, $\mathbf{q}$ represents the heat flux vector per unit surface area and unit time, e represents the internal specific energy, $\hat{\mathbf{S}} = \hat{\mathbf{S}}(\mathbf{F}, T)$ represents the first Piola–Kirchhoff stress tensor [20,22] and $\mathbf{F}$ is the deformation gradient, defined as [20,22]:

$$\mathbf{F} = \mathbf{1} + \nabla \mathbf{u} \tag{2}$$

with $\mathbf{u}$ displacement.

Now we introduce the definition of finite strain tensor $\mathbf{D}$ as follows [20,22]:

$$\mathbf{D} = \frac{1}{2}\left(\mathbf{F}^{+}\,\mathbf{F} - \mathbf{1}\right) = \mathbf{E} + \frac{1}{2}\,\nabla \mathbf{u}^{+}\,\nabla \mathbf{u} \tag{3}$$

where $\mathbf{1}$ is the unit tensor, $\mathbf{F}^{+}$ is the transposed matrix of $\mathbf{F}$, and $\mathbf{E}$ is the infinitesimal strain tensor, defined by the following relation:

$$\mathbf{E} = \frac{1}{2}\left(\nabla \mathbf{u}^{+} + \nabla \mathbf{u}\right) \tag{4}$$

Considering that:

$$\rho\,\dot{e} - \hat{\mathbf{S}} \cdot \dot{\mathbf{F}} = \rho\, c\, \dot{T} - T\,\frac{\partial \mathbf{S}}{\partial T} \cdot \dot{\mathbf{D}} \tag{5}$$

obtained in Refs. [13,14] for an isotropic continuous body [23] under the restriction $\hat{\mathbf{S}}(\mathbf{F}, T) = \mathbf{F}\,\mathbf{S}(\mathbf{D}, T)$ [20,22], Equation (1) can be rewritten as follows [13]:

$$\rho\, c\, \dot{T} = T\,\frac{\partial \mathbf{S}}{\partial T} \cdot \dot{\mathbf{D}} - \nabla \cdot \mathbf{q} + \rho\, r \tag{6}$$

where c is the specific heat. Now we introduce the constitutive equation for an isotropic body [24]:

$$\mathbf{S} = 2\mu\mathbf{E} + \left[\lambda\,\mathrm{tr}\mathbf{E} - \beta\,(T - T_0)\right]\mathbf{1} \tag{7}$$

where λ and μ are the Lamé moduli, which are temperature dependent, tr$\mathbf{E}$ is the trace of the matrix $\mathbf{E}$, $(T - T_0)$ is the temperature variation, while β is defined as [21]:

$$\beta = (3\lambda + 2\mu)\,\alpha \tag{8}$$

where α is the coefficient of linear thermal expansion. Under the assumption of a linear approximation for the gradient displacement, and from its definition in Equation (3), it follows that [13]:

$$\dot{\mathbf{D}} \cong \dot{\mathbf{E}} \tag{9}$$

Thus, from this approximation and the relations (7) and (9), Equation (6) becomes:

$$\rho\, c\, \dot{T} = T\left\{2\,\frac{\partial \mu}{\partial T}\,\mathbf{E} + \left[\frac{\partial \lambda}{\partial T}\,\mathrm{tr}\mathbf{E} - \frac{\partial \beta}{\partial T}\,(T - T_0) - \beta\right]\mathbf{1}\right\} \cdot \dot{\mathbf{E}} - \left(\nabla \cdot \mathbf{q} - \rho\, r\right) \tag{10}$$

Based on experimental [5,24] and theoretical results, we can introduce the following hypothesis [12]:

- The thermodynamic process is adiabatic without any internal heat source: it leads to the following mathematical condition:

$$\nabla \cdot \mathbf{q} - \rho\, r = 0 \tag{11}$$

- The term $(\partial\beta/\partial T)\,(T - T_0)$ is negligible with respect to β, as a consequence of both experimental results [20,24] and the evaluation of the order of magnitude [20],

Consequently, Equation (10) becomes:

$$\rho\, c\, \frac{\dot{T}}{T} = 2\, \frac{\partial \mu}{\partial T}\, \mathbf{E} \cdot \dot{\mathbf{E}} + \left(\frac{\partial \lambda}{\partial T}\, \mathrm{tr}\mathbf{E} - \beta \right) \mathrm{tr}\dot{\mathbf{E}} \tag{12}$$

which represents the differential thermoelastic relationship between temperature and strain.

The constitutive equation, Equation (7) can be inverted, obtaining:

$$\mathbf{E} = \frac{1}{2\mu}\, \mathbf{S} - \left[\frac{\lambda}{2\mu\,(3\lambda + 2\mu)}\, \mathrm{tr}\mathbf{S} + \alpha\,(T - T_0) \right] \mathbf{1} \tag{13}$$

Considering Equation (13) and the following relations among the Lamé constants, λ and μ, the Poisson's ratio ν (Poisson's ratio is a measure of the Poisson effect, i.e., the phenomenon in which a material tends to expand in directions perpendicular to the direction of compression [22]) and the Young's modulus E (Young's modulus is a mechanical property of solid materials that measures the tensile or compressive stiffness when the force is applied lengthwise [22]):

$$\begin{cases} \lambda = \dfrac{E\,\nu}{(1+\nu)\,(1-2\nu)} \\ \mu = \dfrac{E\,\nu}{2\,(1+\nu)} \end{cases} \tag{14}$$

it is possible to obtain the following equation:

$$\frac{\dot{T}}{T} = \left(\Gamma_1\, \mathrm{tr}\mathbf{S} - k_e \right) \mathrm{tr}\dot{\mathbf{S}} + \Gamma_2\, \mathbf{S} \cdot \dot{\mathbf{S}} \tag{15}$$

where

$$\begin{cases} k_e = \dfrac{\alpha}{\rho\, c} \\ \Gamma_1 = \dfrac{1}{\rho\, c} \left(\dfrac{1}{E}\, \dfrac{\partial \nu}{\partial T} - \dfrac{\nu}{E^2}\, \dfrac{\partial E}{\partial T} \right) = \dfrac{1}{\rho\, c}\, \dfrac{\partial}{\partial T} \left(\dfrac{\nu}{E} \right) \\ \Gamma_2 = \dfrac{1}{\rho\, c} \left(\dfrac{1+\nu}{E^2}\, \dfrac{\partial E}{\partial T} - \dfrac{1}{E}\, \dfrac{\partial \nu}{\partial T} \right) = -\dfrac{1}{\rho\, c}\, \dfrac{\partial}{\partial T} \left(\dfrac{1+\nu}{E} \right) \end{cases} \tag{16}$$

The quantity k_e is related to some material properties (density ρ, specific heat c, and linear expansion coefficient α) and represents the ratio between the elastic property and the energy storage capacity of the material. The Γ quantities are related to the thermal variation of the ratio between the elastic deformation and its rigidity weighted on the energy storage capacity of the material.

Now, introducing the usual mathematical-physical notation

$$\begin{cases} \sigma = \mathrm{tr}\mathbf{S} \\ \dot{\sigma} = \mathrm{tr}\dot{\mathbf{S}} \\ \sigma_i = (\mathbf{S})_i \\ \dot{\sigma}_i = (\mathbf{S})_i \end{cases} \tag{17}$$

where $(S)_i$ are the principal stresses with respect to an orthogonal basis $\{e_i\}$, and remembering that [20,22]:

$$\mathbf{S} \cdot \dot{\mathbf{S}} = \sum_{i=1}^{3} (\mathbf{S})_i (\dot{\mathbf{S}})_i \tag{18}$$

it is possible to obtain:

$$\frac{\dot{T}}{T} = \left(\Gamma_1 \sigma - k_e\right) \dot{\sigma} + \Gamma_2 \sum_{i=1}^{3} \sigma_i \dot{\sigma}_i \tag{19}$$

which is the thermoelastic relation between temperature and stress.

To obtain a relationship between temperature and stress, the differential Equation (19) must be considered with the following hypotheses:

- The mass density ρ remains constant throughout the thermodynamic process;
- The partial derivatives of the Poisson's ratio ν and the Young's modulus E with respect to temperature T remain constant over time and temperature.

By means of the above assumptions and using the following notation:

$$\begin{cases} \sigma = \sigma_1 + \sigma_2 + \sigma_3 \\ f = \sigma_1\sigma_2 + \sigma_2\sigma_3 + \sigma_1\sigma_3 \end{cases} \tag{20}$$

with σ and f, respectively, the first and second invariant of the stress tensor, it is possible to integrate the differential temperature–stress Equation (19), obtaining:

$$\ln\left(\frac{T}{T_0}\right) = -k_e\left(\sigma - \sigma_0\right) + \frac{\Gamma_1 + \Gamma_2}{2}\left(\sigma^2 - \sigma_0^2\right) - \Gamma_2\left(f - f_0\right) \tag{21}$$

with σ_0 and f_0 representing the initial values of σ and f.

The result obtained (Equation (21)) is the integral and global temperature–stress relation, in which the right member exhibits a nonlinear dependence on both the first and second invariants of stress, while showing a linear dependence on the second invariant. By assuming that the Poisson's ratio and Young's modulus of elasticity vary with temperature, we can derive a connection between changes in temperature and changes in stress. This relationship includes coefficients that not only denote the thermoelastic constant, as in the Kelvin equation, but also vary based on the average stress, as well as the first and second stress invariants and the modulus of elasticity.

3. Results

Here, the thermal behavior of the elastomers under elastic deformations is considered to be a case study to validate the approach proposed in Section 2. In this analysis, a real mechanical component is loaded with a stress variation. The stress of the elastomer, as a function of time, is expressed by the phenomenological one-dimensional relation [25]:

$$\sigma(\mathrm{Fo}) = \sigma_{eq} + \frac{A}{1 + B\ln(\mathrm{Fo})} \qquad \text{with } \mathrm{Fo} \geq 1 \tag{22}$$

where A, B and σ_{eq} (σ_{eq} is the equilibrium value [25]) are constant, and Fo is the Fourier number. To obtain the temperature variation of the elastomers under elastic deformation, the relation (21) must be used. To do that, the values of the applied stress at $\mathrm{Fo} = 1$ and $\mathrm{Fo} \to \infty$:

$$\begin{cases} \sigma_0 = \sigma(1) = A \\ \sigma_{eq} = \lim\limits_{\mathrm{Fo}\to\infty} \sigma\,\mathrm{Fo} \end{cases} \tag{23}$$

The first relation of the equation's system (23) allows us to obtain the physical meaning of the constant A, which results in the initial stress value.

Now, introducing these values in Equation (21), the thermal behavior of elastomers can be obtained:

$$\ln\left(\frac{T}{T_0}\right) = \left[k_e - \left(\Gamma_1 + \Gamma_2\right)\sigma_{eq}\right] A - \frac{1}{2}\left(\Gamma_1 + \Gamma_2\right) A^2 \tag{24}$$

This last relation represents the temperature variation of elastomer as a consequence of stress variation under elastic deformation. To plot the shape of this relation, it is possible to write it in the following way:

$$\vartheta = \exp\left(\left(\Gamma_1 + \Gamma_2\right)\left(\delta A - \frac{1}{2} A^2\right)\right) \tag{25}$$

where $\vartheta = T/T_0$ and $\delta = \left(\Gamma_1 + \Gamma_2\right)^{-1} k_e - \sigma_{eq}$. The quantity δ is related to some material properties (density ρ, specific heat c and linear expansion coefficient α) but also to the temperature variation of the Poisson's ratio ν and Young's modulus E; consequently, this quantity represents the thermoelastic property of the material concerning the ratio between the elastic deformation and its rigidity. The qualitative shape of the relation (25) can be plotted, by numerical simulations, assuming the normalization condition $\Gamma_1 + \Gamma_2 = 1$:

- In Figure 1, it has been plotted with positive δ values. In this case, the elastomer is also a thermal conductor, and the shape shows that, as a consequence of the applied external stress, its temperature demonstrates a considerable increase;
- In Figure 2, it has been plotted with negative δ values. In this case, the elastomer is not a thermal conductor, and the shape shows that, as a consequence of the applied external stress, its temperature presents a considerable decrease;
- In Figure 3, it has been plotted with zero δ values. This is a particular case in which the thermal behavior compensates for the elastic stress. In this case, the elastomer has similar thermal and elastic behavior for slow values of the applied external stress.

In all three cases, there exists an upper limit of the applied external stress, which represents the physical limit of the elastic behavior of the elastomer: when the applied external stress is greater than this limit, the elastomer structure can be mechanically damaged. This upper limit depends on the kind of elastomer.

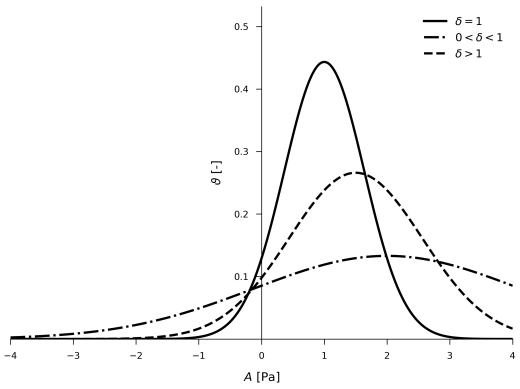

Figure 1. Dimensionless temperature ϑ shape as a function of the applied stress A [Pa] with different positive coefficient, δ [Pa^{-1}], of the first power in the argument of the exponential function in Equation (25). In this scenario, the elastomer acts as a thermal conductor, and the shape shows that, due to the external stress applied, there is a significant rise in its temperature.

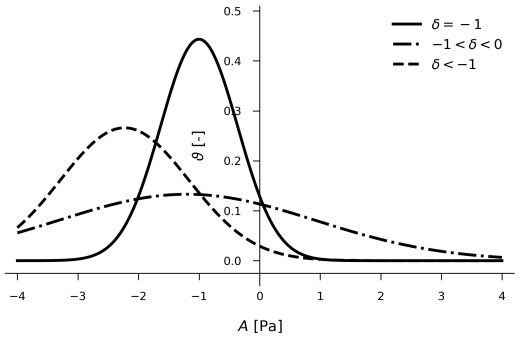

Figure 2. Dimensionless temperature ϑ shape as a function of the applied stress A [Pa] with different negative coefficients, δ [Pa^{-1}], of the first power in the argument of the exponential function in Equation (25). In this scenario, the elastomer does not act as a thermal conductor, and the shape shows that, due to the external stress applied, there is a significant decrease in its temperature.

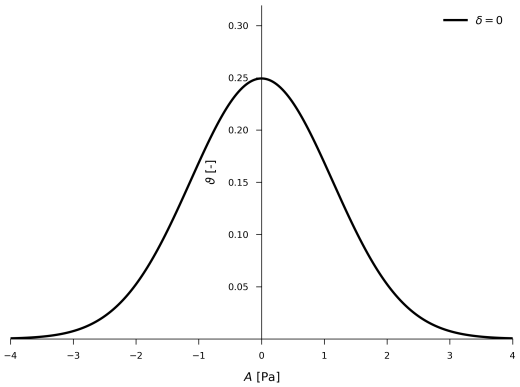

Figure 3. Dimensionless temperature ϑ shape as a function of the applied stress A [Pa] with null coefficient, δ [Pa^{-1}], of the first power in the argument of the exponential function in Equation (25). In this scenario, the elastomer displays comparable thermal and elastic properties at low levels of the applied external stress.

Now, we need to compare our results with experimental data. To do so, we consider the experiment developed by Dippel et al. [26]. In this paper, A natural rubber cubic specimen of 2 mm thickness is pulled in one direction up to a maximum deformation of 10%, which is kept constant for 3600 s. A pre-deformation of 20% was previously applied, and the specimens rested for 24 h at room temperature. The physical properties of the sample are summarized in Table 1.

Table 1. Physical properties of the sample for comparison between the present analytical model and the experimental results. Only the quantities of interest for comparison have been summarized from Ref. [26].

Characteristics	Symbol	Value	Unit of Measurements	Reference
Density	ρ	1.13×10^3	kg m^{-3}	Table 1 of Ref. [26]
Specific heat	c	$784 + 2.47 \cdot T$	J kg^{-1} K^{-1}	Table 1 of Ref. [26]
Reference temperature	T_0	293	K	Ref. [26]
Coefficient of linear thermal expansion	α	2.15×10^{-4}	K^{-1}	Ref. [26]
Thermal conductivity	k_{th}	0.240 (at 20 °C)	W m^{-1} K^{-1}	Figure 4 of Ref. [26]
		0.225 (at 50 °C)	W m^{-1} K^{-1}	Figure 4 of Ref. [26]
		0.222 (at 80 °C)	W m^{-1} K^{-1}	Figure 4 of Ref. [26]

Considering the values in Table 1, the values of k_e are reported in Table 2.

Table 2. Values of k_e in relation to temperature as obtained using the values of Table 1, which summarizes the data reported in Ref. [26].

Symbol	Value	Unit of Measurements	Temperature
k_e	1.26×10^{-7}	Pa^{-1}	20 °C
	1.21×10^{-7}	Pa^{-1}	50 °C
	1.15×10^{-7}	Pa^{-1}	80 °C

To validate the result obtained here, we consider the temperature variation due to self-heat generated during the stress application at 20 °C, 50 °C, and 80 °C, as reported in Ref. [26]. Considering the initial stress values $\sigma_0 = A$ at these temperatures—equal to 0.32 MPa, 0.30 MPa, and 0.27 MPa, respectively [26]—we have evaluated the temperature variation due to self-heating generated during the stress application $\Delta T / T_0$, using Equation (25), such that:

$$\frac{\Delta T}{T} = \frac{T - T_0}{T} = \vartheta - 1 \tag{26}$$

The results obtained are represented in Figure 4 for 20 °C, in Figure 5 for 50 °C, and in Figure 6 for 80 °C. We can highlight that Equation (25) allows us to obtain a similar shape to the plot obtained from experimental data. In Figures 4–6, we have introduced the error bars only for the data calculated by our approach, because the data from the literature were presented without information on the possible error. For our error evaluation, we have used the error propagation method, introducing a maximum theoretical error percentage of 5% for σ. In particular, our focus lies in obtaining the same values of the measured thermophysical quantities at the initial and final stationary state: it is possible to highlight that with the proposed model, we can obtain just these values. We can highlight that the reference shape is always inside the accepted range of our model.

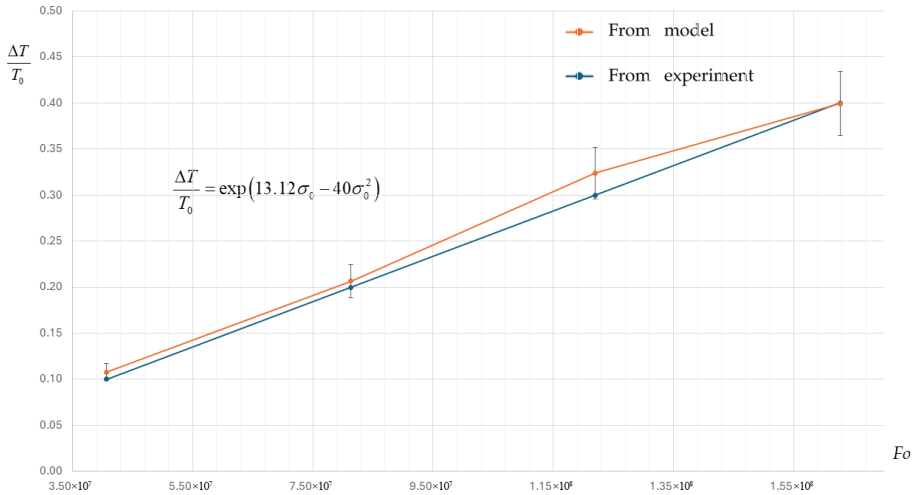

Figure 4. Comparison between the temperature variation ratio at 20 °C over reference temperature from the experimental data reported in Ref. [26] and the model here developed. The R^2 value results 0.9968. In the figure, the axes are expressed in dimensionless quantities of temperature variation ratio and Fourier number.

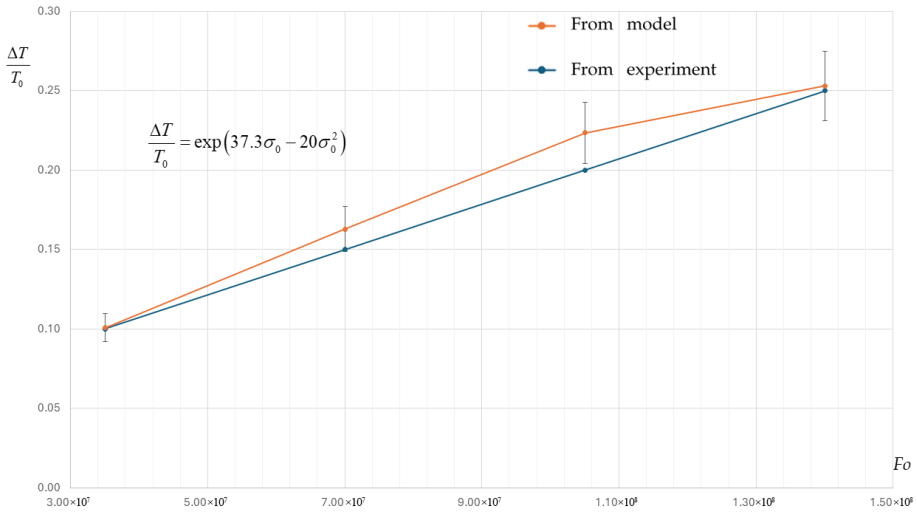

Figure 5. Comparison between the temperature variation ratio at 50 °C over reference temperature from the experimental data reported in Ref. [26] and the model here developed. The R^2 value results 0.9956. In the figure, the axes are expressed in dimensionless quantities of temperature variation ratio and Fourier number.

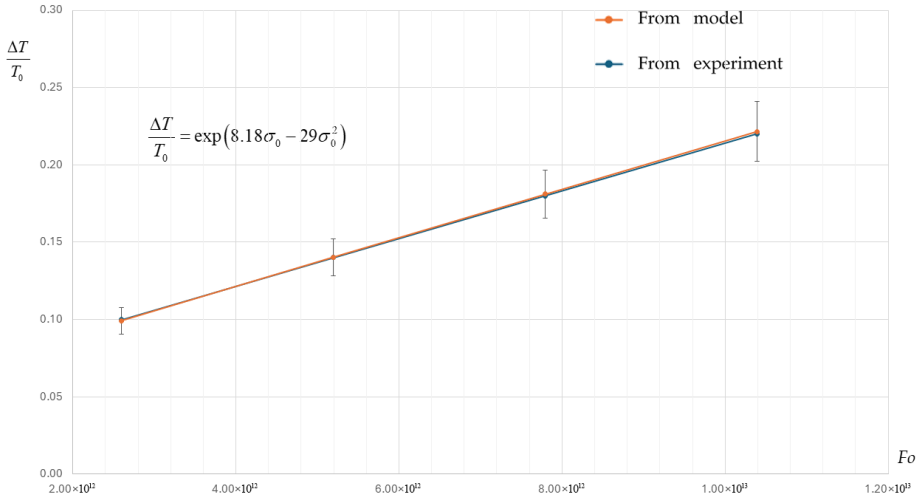

Figure 6. Comparison between the temperature variation ratio at 80 °C over reference temperature from the experimental data reported in Ref. [26] and the model here developed. The R^2 value results 0.9996. In the figure, the axes are expressed in dimensionless quantities: temperature variation ratio and Fourier number.

4. Discussion

A continuum mechanical approach concerning the thermomechanical modelling of rubberlike materials was developed [27–29] to describe the elastic, viscoelastic, and plastic properties of elastomers or thermoplastic polymers, obtaining several equations based on deformation-like quantities [30]. In these studies, the temperature of the material is treated as constant, leading to the formulation of constitutive equations under isothermal conditions, which are thus unaffected by temperature variations. However, in real applications, the temperature results are crucial, as they vary significantly throughout the component's lifespan. Consequently, the mechanical properties change significantly with temperature [26].

The thermoelastic phenomenon (or effect) was originally introduced by Lord Kelvin in 1853 [31]. This effect describes the temperature variation that occurs in materials subjected

to external forces, which in turn vary the material's volume. Specifically, when a material is compressed under a compressive load, its temperature tends to increase, whereas tensile deformation leads to a temperature decrease. As a result, applying a cyclic mechanical load to a component causes a corresponding cyclic oscillation in temperature. Within the elastic regime (elastic condition), these thermal fluctuations are generally small (typically on the order of mK) and thus often neglected in classical elasticity theory. Nonetheless, the development of highly sensitive infrared detection technologies has made it possible to accurately capture these subtle temperature shifts [3].

To guarantee a linear thermoelastic response in experimental observations, the applied loading cycle must occur at a sufficiently high frequency to inhibit heat exchange, thereby approximating adiabatic conditions. True adiabaticity would require either zero thermal conductivity or a complete absence of stress gradients within the specimen, both of which are idealized conditions. Nonetheless, increasing the loading frequency reduces the thermal diffusion length, thus limiting deviations from adiabatic behavior. In contemporary thermoelastic stress analysis (TSA), surface temperature fluctuations induced by cyclic loading are captured using infrared cameras fitted with photon detector arrays. This approach enables the detection of temperature signals that correlate with the mechanical loading cycle. As a result, thermoelastic measurements must be performed under dynamic conditions with appropriately selected loading frequencies to minimize thermal conduction effects to ensure the maintenance of adiabatic conditions, preventing heat transfer through the test piece [3].

The thermal behavior of solids subjected to elastic deformations has been studied to develop a model capable of describing such properties within a classical thermodynamic approximation.

The increasing use of innovative materials (high-tech materials) for structural applications has demonstrated the need for more in-depth studies on their mechanical behavior. Increasing attention has, therefore, been paid to the analysis of the interaction between thermal and mechanical effects in solid bodies [13]. The behavior of solids under the combined effect of external stresses and temperature has considerable practical importance. Even in the ideal case of a perfect crystal, an exhaustive microscopic description of these effects is still missing. Most theoretical studies have focused on the limit of zero temperature, also assuming a perfect and complete crystalline structure. These two assumptions are so restrictive that they allow useful predictions only for relatively small values of temperature and external stress. Instead, for high values of external stress, large-scale defects can be produced, and transformations of the crystalline state can occur.

Recently, the maximum principle for irreversible entropy in open systems has been useful to study the stability of stationary states [13] and has been then applied to the analysis of solid materials, obtaining results in agreement with those obtained from traditional models, but without restrictions and particular assumptions on the physical and chemical conditions of the system.

Additionally, the temperature-related mechanical characteristics of natural rubber filled with carbon black were studied experimentally [26], revealing that the stress-strain response under infinitely slow rates remains unaffected by temperature. However, for finite-time deformations, the mechanical behavior of the material is significantly influenced by temperature [26].

5. Conclusions

Elastomeric components are seeing growing use in a wide range of engineering applications, particularly in load-bearing structures. For such applications, a thorough understanding of the material's mechanical characteristics and properties is essential.

Unlike conventional construction materials such as steel or aluminum, elastomers exhibit pronounced time-dependent behavior, which significantly influences their mechanical response [26].

The diffusion of extremely accurate instrumentation has also fostered the progress of knowledge in this field, used for non-destructive testing of structures, for the measurement of temperatures based on heat emissions from the surfaces of solid bodies [9]. Recent progress in infrared thermography, especially the introduction of infrared staring array radiometric detectors, has paved the way for its application in evaluating fatigue-related damage. A prominent technique leveraging this capability is thermoelastic stress analysis (TSA), which enables the investigation of in-plane stress distributions in solid structures by detecting subtle temperature variations caused by cyclic mechanical loading [3]. From the perspective of fatigue analysis, TSA represents a significant breakthrough compared to other experimental stress analysis methods [32,33]. TSA allows for the direct determination of the stress intensity factor by calculating the cyclic stress field distribution adjacent to the crack tip. This approach provides a means to assess the effective driving force responsible for fatigue crack propagation. Such an advancement is made possible because TSA provides the near-crack-tip stress distribution based on temperature variations observed at the specimen's surface, resulting from the thermoelastic effect. Consequently, TSA offers a direct assessment of the cyclic strains surrounding the crack tip. Thus, the stress pattern observed at the crack tip reflects the specimen's response to the applied loading cycle [3].

In the elastic field, the problem to be addressed is how to analyze the relationships between temperature variations and the variation of the tensor of stresses [5,10,11].

In this work, we have proposed a theoretical approach for a thermophysical model that, based on the study of the properties of the global thermal behavior of solids, can describe the thermodynamic effects of elastic deformations. The model allows us to obtain a good description of the thermal behavior of elastic bodies in relation to the thermal-stress correlation. The result could be useful in the analysis of elastic bodies to determine some thermophysical properties such as the thermal expansion coefficient, the temperature variation of strain tensor, etc., using non-invasive experimental techniques, such as TSA.

Author Contributions: Conceptualization, U.L. and G.G.; methodology, U.L. and G.G.; validation, U.L. and G.G.; formal analysis, U.L.; investigation, U.L. and G.G.; resources, U.L.; data curation, G.G.; writing—original draft preparation, U.L. and G.G.; writing—review and editing, U.L. and G.G.; visualization, G.G.; supervision, U.L.; project administration, U.L.; funding acquisition, U.L. All authors have read and agreed to the published version of the manuscript.

Funding: This research received no external funding.

Institutional Review Board Statement: Not applicable.

Informed Consent Statement: Not applicable.

Data Availability Statement: The original contributions presented in this study are included in the article. Further inquiries can be directed to the corresponding author.

Conflicts of Interest: The authors declare no conflict of interest.

Nomenclature

Symbol	Quantity	Unit of measurements
Latin letters		
$a = k_{th}/\rho\, c$	thermal diffusivity	$m^2\ s^{-1}$
A	coefficient	Pa
c	specific heat	$J\ kg^{-1}\ K^{-1}$
$\mathbf{D}$	finite strain tensor	[-]

e	specific internal energy per unit time	J kg^{-1}
E	Young's modulus	Pa
$\mathbf{E}$	infinitesimal strain tensor	[-]
f	second invariant of the stress tensor	Pa^2
$\mathbf{F}$	deformation tensor	[-]
$\mathbf{G}$	metric tensor	[-]
$\mathbf{h}$	reference axis vector	[-]
k_e	coefficient	Pa^{-1}
L	length	m
m	mass	kg
p	pressure	Pa
$\mathbf{q}$	heat flux, i.e., heat power per unit area	W m^{-2}
r	heat supply per unit mass and unit time	W kg^{-1}
$\mathbf{r}$	position	m
$\mathbf{s}$	coordinates vector	m
$\mathbf{S}$	the first Piola–Kirchhoff stress tensor	J m^{-3}
T	temperature	K
$\mathbf{u}$	displacement	m
V	total interaction potential	V
Greek letters		
α	coefficient of linear thermal expansion	K^{-1}
β	coefficient	Pa K^{-1}
δ	coefficient	Pa^{-1}
ϕ	electrostatic potential	V
Γ_1	coefficient	Pa^{-2}
Γ_2	coefficient	Pa^{-2}
λ	Lamé modulus	Pa
η	specific entropy	J kg^{-1}
μ	Lamé modulus	Pa
ν	Poisson's ratio	[-]
ρ	mass density	kg m^{-3}
Ω	volume	m^3
σ	first invariant of the stress tensor	Pa
ϑ	adimensional temperature	[-]
Θ	specific Helmholtz free energy	J kg^{-1}
Symbols		
$\dot{()}$	the first order time differential	
$\ddot{()}$	the second order time differential	
0	reference state (environment)	
el	elastic	
Fo $= at/L^2$	Fourier number	[-]

References

1. Gidiagba, J.O.; Daraojimba, C.; Ofonagoro, K.A.; Eyo-Udo, N.L.; Egbokhaebho, B.A.; Ogunjobi, O.A.; Banso, A.A. Economic Impacts and Innovations in Materials Science: A Holistic Exploration of Nanotechnology and Advanced Materials. *Eng. Sci. Technol. J.* **2023**, *4*, 84–100. [CrossRef]
2. Moshood, T.D.; Nawanir, G.; Mahmud, F.; Mohamad, F.; Ahmad, M.H.; AbdulGhani, A. Sustainability of biodegradable plastics: New problem or solution to solve the global plastic pollution? *Curr. Res. Green Sustain. Chem.* **2022**, *5*, 100273. [CrossRef]
3. Díaz, F.A.; Patterson, E.A.; Yates, J.R. Application of thermoelastic stress analysis for the experimental evaluation of the effective stress intensity factor. *Fract. Struct. Integr.* **2013**, *7*, 109–116. [CrossRef]
4. James, M.N. Some unresolved issues with fatigue crack closure measurement, mechanisms and interpretation problems. In *Advance in Fracture Research, Proceedings of the 9th International Conference on Fracture, Sydney, Australia, 1–5 April 1997*; Karihaloo, B.L., Mai, Y.W., Ripley, M.I., Ritchie, R.O., Eds.; Pergamon Press: Oxford, UK, 1997; pp. 2403–24149.

5. Berra, M.; Bocca, P. Thermoelastic stress analysis: Temperature-strain relationships in concrete and mortar. *Mater. Struct.* **1993**, *26*, 395–404. [CrossRef]
6. Sih, G.; Tzou, D. Irreversibility and damage of SAFC-40R steel specimen in uniaxial tension. *Theor. Appl. Fract. Mech.* **1987**, *7*, 23–30. [CrossRef]
7. Beghi, M.; Berra, M.; Caglioti, G.; Fazzi, A. A thermoelastic method to measure the thermal expansion coefficient. *Mater. Struct.* **1986**, *19*, 65–69. [CrossRef]
8. Stanley, P.; Chan, W.K. A New Experimental Stress Analysis Technique of Wide Application. In *Experimental Stress Analysis*; Springer: Dordrecht, The Netherlands, 1986; pp. 479–487. [CrossRef]
9. Wong, A.; Sparrow, J.; Dunn, S. On the revised theory of the thermoelastic effect. *J. Phys. Chem. Solids* **1988**, *49*, 395–400. [CrossRef]
10. Ryall, T.; Wong, A. Determining stress components from the thermoelastic data—A theoretical study. *Mech. Mater.* **1988**, *7*, 205–214. [CrossRef]
11. Huang, Y.M.; Rowlands, R.E.; Lesniak, J.R. Simultaneous stress separation, smoothing of measured thermoelastic isopachic information and enhanced boundary data. *Exp. Mech.* **1990**, *30*, 398–403. [CrossRef]
12. Lucia, U. Statistical approach of the irreversible entropy variation. *Phys. A Stat. Mech. Its Appl.* **2008**, *387*, 3454–3460. [CrossRef]
13. Bonadies, M.; Lucia, U.; Patrone, F. Thermoelastic stress analysis for linear thermoelastic bodies. *Quad. Dip. Mat. Torino* **1998**, *1*, 1–15.
14. Bonadies, M. Thermoelastic Stress Analysis for Linear Thermoelastic Bodies. *Rend. Semin. Mat. Dell'Univ. Politec. Torino* **2007**, *65*, 231–239.
15. Shakeriaski, F.; Ghodrat, M.; Escobedo-Diaz, J.; Behnia, M. Recent advances in generalized thermoelasticity theory and the modified models: A review. *J. Comput. Des. Eng.* **2021**, *8*, 15–35. [CrossRef]
16. Maxwell, J.C. IV. On the dynamical theory of gases. *Philos. Trans. R. Soc. Lond.* **1867**, *157*, 49–88. [CrossRef]
17. Lord, H.; Shulman, Y. A generalized dynamical theory of thermoelasticity. *J. Mech. Phys. Solids* **1967**, *15*, 299–309. [CrossRef]
18. Green, A.E.; Lindsay, K.A. Thermoelasticity. *J. Elast.* **1972**, *2*, 1–7. [CrossRef]
19. Green, A.E.; Naghdi, P.M. Thermoelasticity without energy dissipation. *J. Elast.* **1993**, *31*, 189–208. [CrossRef]
20. Carlson, D.E. Linear Thermoelasticity. In *Linear Theories of Elasticity and Thermoelasticity: Linear and Nonlinear Theories of Rods, Plates, and Shells*; Truesdell, C., Ed.; Springer: Berlin/Heidelberg, Germany, 1973; pp. 297–345. [CrossRef]
21. Boyle, J.T.; Cummings, W.M. Finite Element Analysis of Spate Benchmarks. In *Applied Stress Analysis*; Hyde, T.H., Ollerton, E., Eds.; Springer: Dordrecht, The Netherlands, 1990; pp. 150–159. [CrossRef]
22. Gurtin, M.E. The Linear Theory of Elasticity. In *Encyclopedia of Physics (Mechanics of Solids II)*; Flügge, S., Truesdell, C., Eds.; Springer: Berlin, Germany, 1972; Volume VI a/2, pp. 1–295.
23. Ivanova, J.; Bontcheva, N.; Pastrone, F.; Bonadies, M. Thermoelastic Stress Analysis for Linear Elastic Bodies. In Proceedings of the Vibration Problems ICOVP 2005, Istanbul, Turkey, 5–9 September 2005; İnan, E., Kırış, A., Eds.; Springer: Dordrecht, The Netherlands, 2007; pp. 243–248.
24. Wong, A.; Jones, R.; Sparrow, J. Thermoelastic constant or thermoelastic parameter? *J. Phys. Chem. Solids* **1987**, *48*, 749–753. [CrossRef]
25. Clarke, S.M.; Terentjev, E.M. Slow Stress Relaxation in Randomly Disordered Nematic Elastomers and Gels. *Phys. Rev. Lett.* **1998**, *81*, 4436–4439. [CrossRef]
26. Dippel, B.; Johlitz, M.; Lion, A. Thermo-mechanical couplings in elastomers—Experiments and modelling. *ZAMM—J. Appl. Math. Mech./Z. Angew. Math. Mech.* **2014**, *95*, 1117–1128. [CrossRef]
27. Treloar, L.R.G. The mechanics of rubber elasticity. *Proc. R. Soc. Lond. A Math. Phys. Sci.* **1976**, *351*, 301–330. [CrossRef]
28. Coleman, B.D.; Noll, W. The thermodynamics of elastic materials with heat conduction and viscosity. *Arch. Ration. Mech. Anal.* **1963**, *13*, 167–178. [CrossRef]
29. Reese, S.; Wriggers, P. A material model for rubber-like polymers exhibiting plastic deformation: Computational aspects and a comparison with experimental results. *Comput. Methods Appl. Mech. Eng.* **1997**, *148*, 279–298. [CrossRef]
30. Mooney, M. A Theory of Large Elastic Deformation. *J. Appl. Phys.* **1940**, *11*, 582–592. [CrossRef]
31. Thomson, W. On the Thermoelastic, Thermomagnetic and Pyro-electric Properties of Matters. *Philos. Mag.* **1878**, *5*, 4–27. [CrossRef]
32. Díaz, F.A.; Yates, J.R.; Patterson, E.A. Some improvements in the analysis of fatigue cracks using thermoelasticity. *Int. J. Fatigue* **2004**, *26*, 365–376. [CrossRef]
33. Díaz, F.A.; Patterson, E.A.; Tomlinson, R.A.; Yates, J.R. Measuring stress intensity factors during fatigue crack growth using thermoelasticity. *Fatigue Fract. Eng. Mater. Struct.* **2004**, *27*, 571–584. [CrossRef]